Measuring Synchronization for coupled systems using Visibility Graph Similarity

AyanMitra, BudhadityaPyne

Abstract*—Synchronization is defined as interdependencies among two or more time series. Recent advances on information theory and non-linear dynamical systems has allowed us to investigate different types of synchronization measures on different time series data such Electroencephalogram (EEG), Magnetoencephalogram (MEG) and other non-stationary signals.However,these kind of statistical interdependencies are also prominently observed in the coupled chaotic systems occurring in nature. In most coupled systems the internal variants and the interdependencies among their subsystems are not accessible. Therefore, to measure the statistical interdependencies among the coupled systems, different non-linear approaches has been adopted thateffectively determines the amount of synchronization between the dynamical systems under investigation. In this paper the recently proposed synchronization measurement performance of the Visibility Graph Similarity (VGS)10,11 is computed for two coupled identical Hénon map, two non-identical coupled rössler and Lorenz system over the entire time domain & also compared against linear correlation to estimate the superiority of the method.

***Index Terms*—Coupled model systems, Dynamic systems, Nonlinear system, Synchronization.**

I. INTRODUCTION

The study Synchronization between dynamical systems has been an active field of study for last two decades. Synchronization phenomena in chaotic systems have attracted muchattention in the fields of nonlinear dynamical systems and havefound applications in areas such as laser dynamics, solid state physics, electronics, biology and communication.

In most coupled systems the interdependencies among their subsystems are not easily accessible. For this purpose, cross correlation and coherence functions have been used to measure the interdependency between two time series in terms of time and frequency, respectively. These two measures, however, detect only the linear interdependencies.

In order to overcome the aforementioned deficiency, a new and effective method, called Visibility Graph Similarity (VGS) is proposed in 10,11.VGS is a methodbased on the concept of generalized synchronization and detectsnonlinear and linear dependencies between two signals.VGS relies on the detection of simultaneouslyoccurring patterns, which can be complex and widely different in thetwo signals. The Visibility Graph (VG) can efficiently convert time series to a graph where the order of the VG's vertexes (nodes) is the same as the order of sample times of the time series. It is shown in10, 11 that the topology of the VG of a time series is related to complexity and fractality of the time series.

In the rest of the paper the performance of VGS on effectively determining the interdependencies of dynamical systems is computed on different chaotic systems like coupled identical Hénon map, non-identical coupled rössler and Lorenz system which are also used by T. Kreuzet. al in 7 for comparing different approaches of synchronization on coupled chaotic systems.The variation of synchronization index against coupling coefficient& signal to noise ratio is computed by VGS for all three coupled chaotic systems & their results are also compared against linear correlation since VGS effectively computes cross-correlation among Degree Sequences (DS) of the nodes of the visibility graph.

Manuscript received on August, 2012

AyanMitra, Department of Electrical Engineering, Jadavpur University,Jadavpur, Kolkata, India.

BudhadityaPyne, Department of Electrical Engineering, Jadavpur University, Kolkata, India.

II. VISIBILITY GRAPH SIMILARITY

The determination of Visibility Graph Synchronization is a 6 step process as mentioned in 10,11.

A. *Reconstruction of trajectories in a state space.*

The Visibility Graph Similarity (VGS) attempts to compute the number of similar patterns in time series of the coupled systems which are repeated concurrently. The measurement of similarity is a statistical likelihood with a logical decision making that just determines how much the patterns are similar to one another to a set threshold value irrespective of how much actual similarity actually exists between them. All generalized synchronization including the visibility graph similarity method under considerationrequire reconstruction of trajectories in a state space based on the chaos theory and Takens reconstruction of a time series to measure the interdependencies of the dynamics of the systems which generate the time series. Reconstruction of trajectories based on the chaos theory requires the determination of a time delay or lag time (T) and an embedding dimension (d) to create the state space. In such a state space the nth state, $X_{k,n}$, of the kth trajectory, $X_{k,}$ is represented as follows:

$X_{k,n}= x_{k,n}$, $x_{k,n+T}$, $x_{k,n+2T}$, ……,$x_{k,n+(d-1)T}$

where$x_{k,n}$ is the nth point of the k^{th} time series (k = 1, 2, . . . ,M); when M time series or systems are coupled together). Therefore, each trajectory contains N = R − (d − 1)T states; where R is the number of sampling points of each time series. The time delay and embedding dimension are determined so that the reconstructed trajectories in the new state space are not folded to avoid loss of information. In VGS studies, d and T are taken to be the same for all thetime series in order to be able to compare the similarity of their states.

B. *Creating the Distance Time Series (DTS)*

For each trajectory, X_k, the similarity of the states is determined by comparison with a reference state ($X_{k,n}$) which is the centre state of a preselected window W_{w2}^{w1} (k,n). Window W_{w2}^{w1}(k, n) contains two distinct sequences of states belonging to the same trajectory: [$X_{k,n-w2}$, . . . , $X_{k,n-w1}$] and [$X_{k,n+w1}$, . . . , $X_{k,n+w2}$]. Indeed, the window W_{w2}^{w1} (k, n). around the reference state,

$X_{k,n}$, contains all states, $X_{k,m}$, whose index, m, satisfies the condition: $w1 < |n - m| < w2$. w1 is the Theiler correction 16 used to prevent information redundancy in the similarity computation. The number of states restricted in the window is $2(w2 - w1)$, called the width of thewindow, and w2 is an integer number which determines the maximum temporal distance that a state can have from the reference state.

C. Constructing Visibility Graph (VG)

The VG of the time series x is constructed in the following manner: consider the i^{th} node of the graph, a_i, corresponds to the i^{th} point of the time series, x_i. Two vertexes (nodes) of the graph, a_m and a_n, are connected via a unidirectional edge if and only if:

$$x_{m+j} < x_n + \left(\frac{n-(m+j)}{(n-m)}\right)(x_m - x_n) \; ; \forall j \in Z+; \; j<n-m$$

a_i is the ith vertex of the graph corresponding to xi. If and only if x_i and x_j can see each other, the corresponding vertexes of the VG, a_i and a_j, connect together through a bidirectional edge.

D. Finding the Degree Sequence (DS)

In un-weighted graphs, the number of edges connected to a node is called the degree of that node. Degrees of the nodes of a VG obtained from DTSs are sequences of degrees of their nodes (one DS for each DTS).

E. Computing the cross correlation between the DSs

Similarities of dynamics of the coupled systems (in a window) are obtained through computing similarity of the trajectories (in that window). The similarity of the DSs are evaluated by evaluating the cross-correlation function:

$$S[DS(X),DS(Y)] = \left(\frac{\text{cov}\,(DS(X),DS(Y))}{\sigma(X)*\sigma(Y)}\right)$$

where DS(X) is DS of the trajectory X falling in the window $W_{w2}^{w1}(k, n)$, |x| indicates the absolute value of x, cov[x, y] is the covariance of x and y, and σ(x) is the standard deviation of x. Since the VG of a time series preserves its time ordering, similarity of the dynamics of two time series indeed is a measure of their synchronization.

F. Averaging similarities in terms of shifting the window

The window$W_{w2}^{w1}(k, n)$ is shifted (with shorter steps for higher temporal resolution but with a higher computational load) and similarity of the dynamics is computed in each window. Then, the overall synchronization of the coupled systems is calculated through averaging the computed synchronizations over all windows. That will be the VGS.

III. Evaluation & Results

A. Dependence on Coupling Strength

In this example, values of 3 and 5 were used for the embedding dimension (d) and lag time (T), respectively. w2 was taken as 50. The term w1, known as the Theiler correction, is used to reduce the likelihood of the vectors (states) representing a recurrence of the reference state ($X_{k,n}$) in order to avoid pseudo-similarities that may be not related to the dynamic system. Montez et al. 8 suggest a value of $T(d - 1)$ for w1 to avoid overlap between the reference state and other states. Using this equation yields a value of 9 for w1 which is the value used in this research. The initial values of variables of the model all the models were taken in the range [-1, 1]. The coupling parameter (c) was varied from 0 to 1 for coupled Hénon map & 0 to 2 for Lorenz &Rössler systems in increments of 0.1, and the VGS were computed for each value of the coupling parameter c. Since the VGS effectively computes the linear correlation among the degree sequences so the variation of synchronization against coupling coefficient is also plotted for linear correlation.

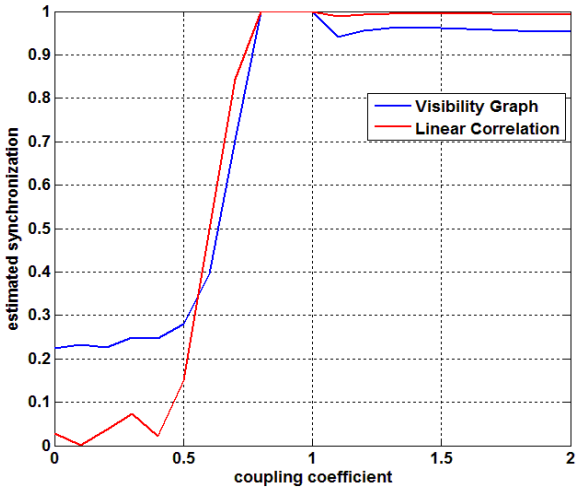

Fig.1. Comparison of Visibility graph similarity & linear correlation against coupling strength for ideantical coupled hénon map

For the coupled Hénon system the VGS starts from 0.2 whereas the linear correlation starts from very low value as 0.3. There is a sudden peak for C=0.3 for both the Visibility Graph Similarity & linear correlation. Both the measures show sharp rise after C=0.6 indicating high correlation for coupled hénon system however their values almost saturate for C>0.8. Its notable that for VGS the synchronization value decreases after C=1 denoting gradual loss in synchronization however this loss of synchronization is not detectable for linear correlation.

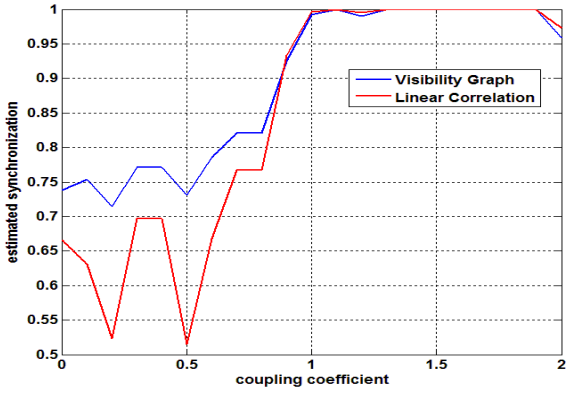

Fig.2. Comparison of Visibility graph similarity & linear correlation against coupling strength for coupled Lorenz systems

For coupled Lorenz system

abrupt loss of synchronization is visible for C=0.2 & C=0.5 as shown by both VGS & Linear correlation however the value reached by linear correlation is very less. The variation of Synchronization is monotonic after C>0.5. However a sharp rise is shown by both VGS & Linear correlation for transition from C=0.9 to C=1. There is also complete synchronization for $1.3 \leq C \leq 1.9$ as shown by both themeasures. But a loss of synchronization can be observed by both measures for C=2.

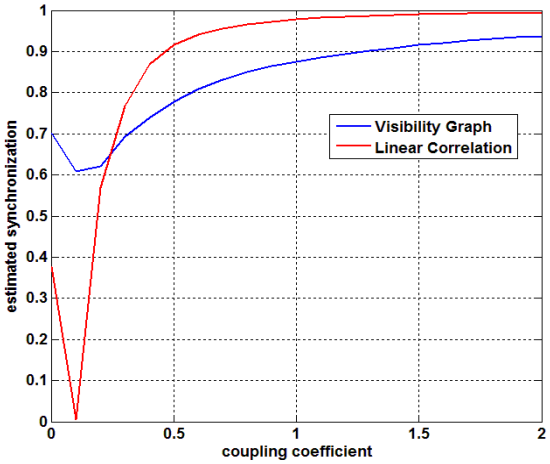

Fig.3. Comparison of Visibility graph similarity & linear correlation against coupling strength for coupled Rössler systems

For coupled Rössler system there is a high value of synchronization for C=0. Expect for this aberration the variation ofsynchronization with coupling coefficient isstrictlymonotonicas shown by both measures. The linear correlation reaches the value of 0 for C=0.1 showing a complete loss of synchronization. However unlike coupled Hénon map & coupled Lorenz system, the value of synchronization by VGS never reaches 1 in the range of $0 \leq C \leq 2$. But for the linear correlation synchronization value reaches 1 for C=2 denoting complete synchronization for coupled Rössler system.

B. Robustness against noise

To evaluate the robustness against noise for different synchronization measures, the study design used by T. Kreuzet. al7is adopted here. The signal-to-noise ratio defined as $R= \sigma_{signal}/\sigma_{noise}$(with σ_{noise} and σ_{signal} denoting the standard deviations ofnoise and signal, respectively), is used as a second controlparameter along with coupling coefficient. For each coupled model system, this noise-to-signal ratio was increased according to the values used by as follows:

$$R=10^{(-2+0.1q)} \text{with } q = 0,1, \ldots, 30.$$

thereby covering the range from 0.01 to 10 equidistantly on alogarithmic scale

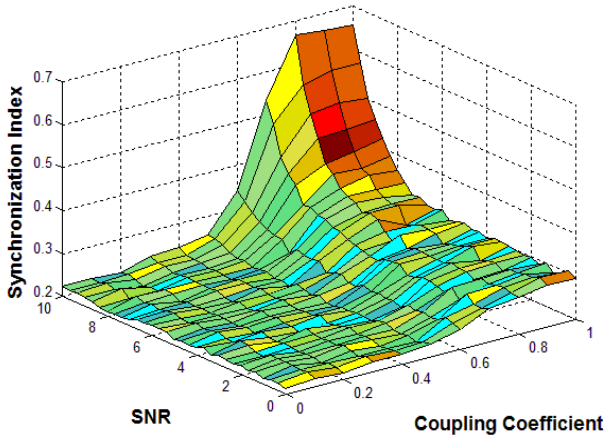

Fig. 4. Color-coded dependence on the coupling strength and the noise-to-signal ratio for Gaussian white noise by visibility Graph similarity for coupled hénon system

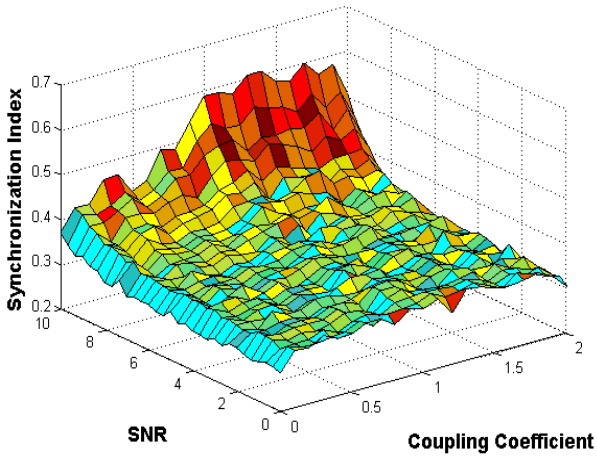

Fig. 5. Color-coded dependence on the coupling strength and the noise-to-signal ratio for Gaussian white noise by visibility Graph similarity for coupled Lorenz system

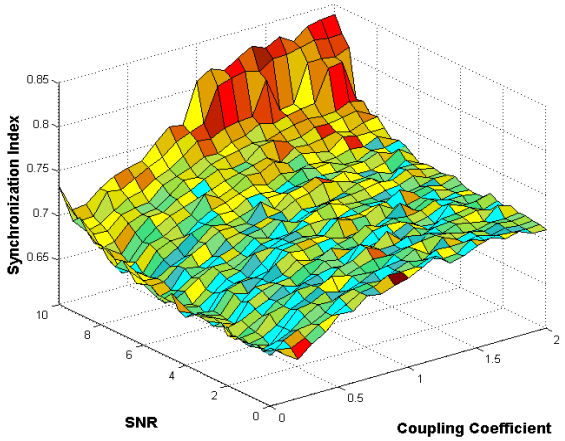

Fig. 6. Color-coded dependence on the coupling strength and the noise-to-signal ratio for Gaussian white noise by visibility Graph similarity for coupled Rössler system

For all coupled systems, the decrease the signal-to-noise ratio leads to a gradual masking of the dependence on the coupling strength. For the minimum signal-to-noise ratio R = 0.01 all measures attain rather constant values close to the levels obtained for uncoupled systems without noise.

For coupled hénon systems a sharp rise in VGS can be observed for C=0.7 & SNR=7 however for both measures the synchronization value remains almost constant for C>0.8 irrespective of change in noise level for 0≤SNR≤6.

For coupled Lorenz system both measures yield almost constant value of synchronization for $1 \leq C \leq 1.9$ &0 ≤SNR≤8. However for C=2 there is a sudden decrease in synchronization index as depicted in fig.6.

For coupled Rössler system, the variation of synchronization with variation of SNR is very less denoting highest amount of robustness against noise among all the coupled systems followed by Lorenz system & then Hénon map.

IV. DISCUSSION

The aim of this study was to perform a comparison of Visibility Graph Similarity against linear correlation on model

systems.One of the assumptions for our study was that an effective synchronization measurement should be sensitive to the coupling parameter but affected less by the inner parameters and dynamics of the individual systems which are not related to the coupling. To this end we compared different measures regarding their capability to reflect different degrees of coupling between two model systems both with presence & absence of noise.Despite some caveats, the variation of synchronization showcased an overall monotonic characteristic with increase of coupling coefficient & signal-to-noise ratio.

V. CONCLUSION

We have applied a linear & a non-linear measure of synchronization to coupled chaotic systems. However the variation of synchronization index for linear correlation measure for all the coupled under consideration displayed very abrupt rise after a certain value of coupling coefficient. On the other hand, the increase of synchronization index was less abrupt as they showed comparatively high value of synchronization even at low values of coupling coefficient. It is also interesting to note that different coupled systems displayed different response of synchronization index of visibility graph similarity to the inclusion of noise. So in many cases like synchronization of EEG signals the visibility graph similarity is now preferred over other linear measures like linear correlation as it captures the dynamics of the systems more effectively.

VI. ACKNOWLEDGMENTS

We are very thankful to Dr. Thomas Kreuz from Institute of Complex Systems, Florence, Italy for providing some programs which were very crucial to simulate one of the coupled systems used in our analysis. One of us (AyanMitra) would also like to acknowledge the support of Dr. AurobindaRoutray from Department of Electrical Engineering, IIT Kharagpur to conduct a research project on synchronization of non-stationary signals.

APPENDIX

In our analysis six measures of synchronization are applied to time series (length N = 2000) of three coupled model systems.

A. *Coupled Hénon systems*

The first coupling scheme consists of two uni-directionally coupledHénon maps. The equations of motion for the driver and the responder read

$$x_{t+1} = 1\text{-}1.4x_t^2 + 0.3u_t$$
$$u_{t+1} = x_t$$
$$y_{t+1} = 1\text{-}1.4(Cx_t + (1\text{-}C)y_t)y_t + Bv_t$$
$$v_{t+1} = y_t$$

where the parameter C is the coupling parameter which varies from 0 (indicating the subsystems are completely independent) to 1 (indicating the subsystems are completely synchronized). Variable t is discrete time or iteration index, and parameter B determines whether the two subsystems are identical (when B=0.3) or non-identical (when B ≠ 0.3). For our case only identical hénon system were considered.

For coupled hénon system the distribution of values in Driver & responder has quite a chaotic distribution for C= 0 & C=0.5 as depicted in Fig. 8 however the distribution is quite linear for C=0.8. Ultimately for C=1 the distribution almost completely linear denoting complete synchronization.

B. *Coupled Lorenz system*

The second coupling scheme consists of two uni-directionally

coupled Lorenz systems as used by T. Kreuz et. al7 in their study design. The equations of motion for the driver and the responder read:

$$\dot{x}_1 = 10(x_2 - x_1)$$
$$\dot{x}_2 = x_1(28 - x_3) - x_2$$
$$\dot{x}_3 = x_1x_2 - 8/3x_3$$
$$\dot{y}_1 = 10(y_2 - y_1)$$
$$\dot{y}_2 = y_1(28.001 - y_3) - y_2$$
$$\dot{y}_3 = y_1\, y_2 - 8/3y_3 + C(x_3 - y_3).$$

The equations were integrated using Runge–Kutta 4th order with a step size of 0.001 and a sampling interval of 0.01. Note the small parameter mismatch introduced in the second component. The coupling strength C was varied from 0 to 2 in steps of 0.1. For the Lorenz systems the transition towards a synchronized state takes place for C around 1.4.

For coupled Lorenz system the distribution of values in Driver & responder has quite a chaotic distribution for C= 0 depicted in Fig. 9 however the distribution is quite linear for C=1.2. Ultimately for C=2 the distribution almost completely linear denoting complete synchronization. But a loss of synchronization can be witnessed for C=2.

C. *Coupled Rössler systems*

For the two Rössler systems the same diffusive coupling scheme as for the Lorenz systems was used similar to those used by T. Kreuzet. al7 in their study design. The equations of motion of this coupling scheme read:

$\dot{x}_1 = -\omega_x x_2 - x_3$
$\dot{x}_2 = \omega_x x_1 + 0.15x_2$
$\dot{x}_3 = 0.2 + x_3(x_1 - 10)$
$\dot{y}_1 = -\omega_y y_2 - y_3 + C(x_1 - y_1)$
$\dot{y}_2 = \omega_y y_1 + 0.15y_2$
$\dot{y}_3 = 0.2 + y_3(y_1 - 10)$.

The equations were integrated using Runge–Kutta 4th order with a step size of 0.05 and a sampling interval of 0.3. A parameter mismatch between the two systems was introduced by setting $\omega_x = 0.95$ and $\omega_y = 1.05$. The coupling strength C was varied from 0 to 2 in steps of 0.1.
For coupled Rössler system the distribution of values in Driver & responder has quite a chaotic distribution for C= 0 in Fig. 10 however the distribution is quite linear for C=1.2& 1.5. Ultimately for C=2 the distribution almost linear denoting high synchronization.

Unlike Hénon or Lorenz coupled systems the distribution of values of driver & responder never reaches a single straight line due to parameter mismatch intentionally introduced for solving the coupled differential equations.

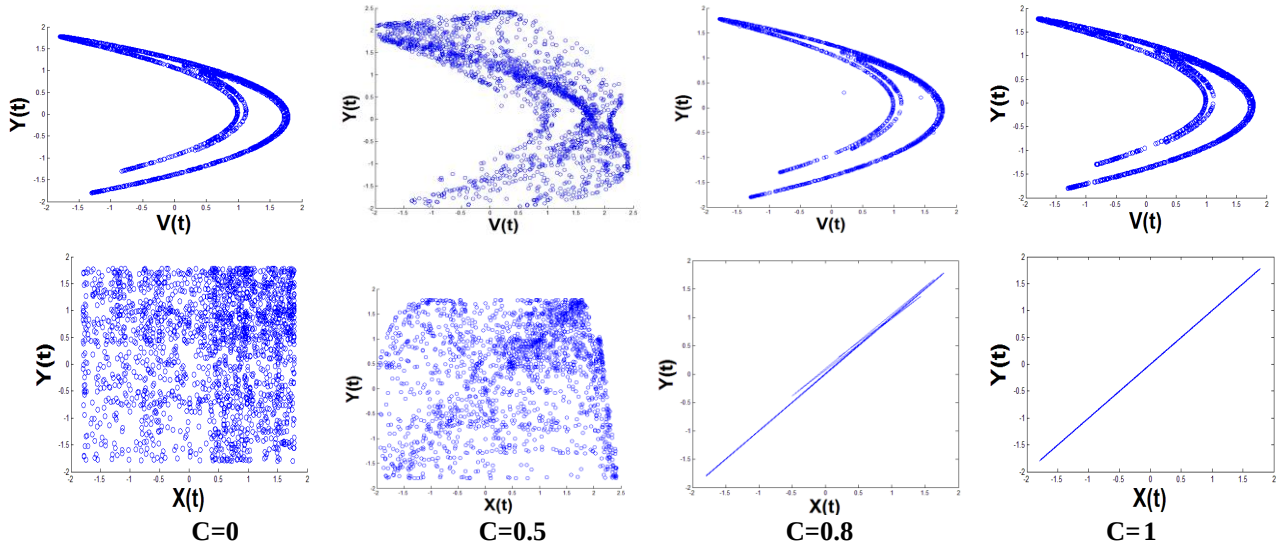

Fig.7. Coupled identical Hénon maps for different coupling strengths C,For each coupling strength the first component of the driver is plotted versus the first component of the responder at the top, whereas at bottom the attractor of the responder is depicted.

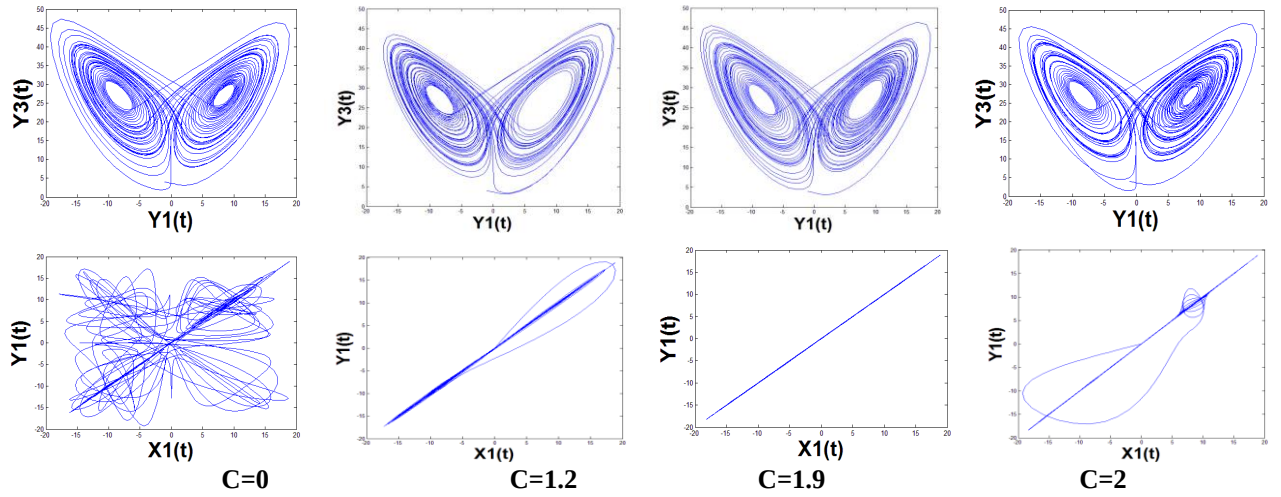

Fig.8. Coupled lorenz systems for different coupling strengths C, For each coupling strength the attractor of the responder (projection on the first and the second component) is depicted at the top, whereas below the first component of the driver is plotted versus the first component of the responder.

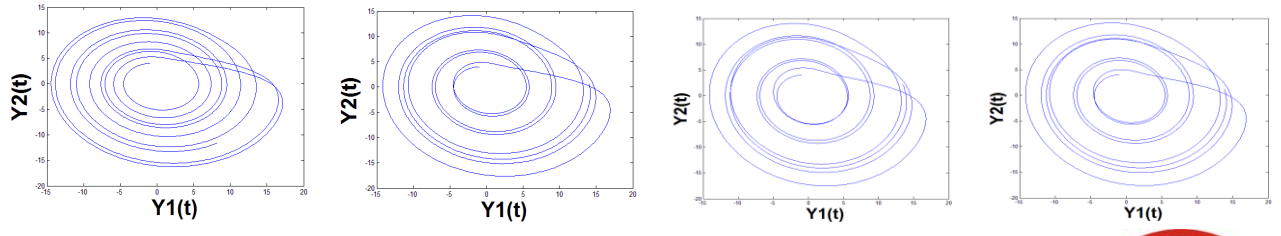

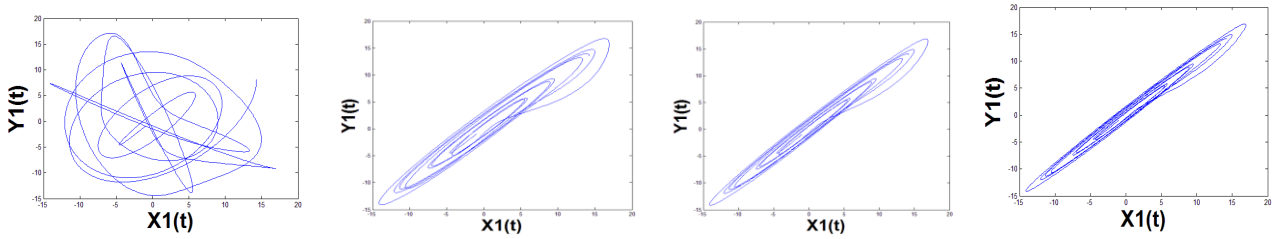

C=0 **C=1** **C=1.5** **C=2**

Fig.9. Coupled Rösler systems for different coupling strengths C, For each coupling strength the attractor of the responder(projection on the first and the second component) is depicted at the top, whereas below the first component of the driver is plotted versus the first component of the responder.

REFERENCES

1. Y. Tang, Q. Miao, J.A. Fang, Synchronization of stochastic delayed chaotic neuralnetworks with Markovian switching and application in communication, Int. J.Neural Syst. 19 (1) (2009) 43–56.
2. J.A. White, C.C. Chow, J. Ritt, C. Soto-Trevino, N. Kopell, Synchronization andoscillatory dynamics in heterogeneous, mutually inhibited neurons, J. Comput. Neurosci. 5 (1) (1998) 5–16.
3. H. V.S. Chakravarthy, N. Gupte, S. Yogesh, A. Salhotra, Chaotic synchronizationusing a network of neural oscillators, Int. J. Neural Syst. 18 (2) (2008) 157–164.
4. L.B. Good, S. Sabesan, S.T. Marsh, K.S. Tsakalis, L.D. Iasemidis, Control ofsynchronization of brain dynamics leads to control of epileptic seizures inrodents, Int. J. Neural Syst. 19 (3) (2009) 173–196.
5. C.J. Stam, B.W. van Dijk, Physica D 163 (2002) 236.
6. R.Q. Quiroga, J. Arnhold, P. Grassberger, Phys. Rev. E 61 (2000) 5142.
7. T. Kreuz, F. Mormann, R.G. Andrzejak, A. Kraskov, K. Lehnertz, P. Grassberger, Measuring synchronization in coupled model systems: a comparison of different approaches, Physica D 225 (1) (2007) 29–42.
8. T. Montez, K. Linkenkaer-Hansen, B.W. van Dijk, C.J. Stam, Synchronization likelihood with explicit time–frequency priors, NeuroImage 33 (4) (2006) 1117–1125.
9. J. Bhattacharya, E. Pereda, H. Petsche, Effective detection of coupling in short and noisy bivariate data, IEEE Trans. Syst. Man Cybern. 33 (1) (2003) 85–95.
10. M. Ahmadlou, H. Adeli, A. Adeli, New diagnostic EEG markers of the Alzheimer's disease using visibility graph, J. Neural Transm. 117 (9) (2010) 1099–1109.
11. MehranAhmadlou, HojjatAdeli, Visibility graph similarity: A new measure of generalized synchronization in coupled dynamic systems, Physica D: Nonlinear Phenomena, Volume 241, Issue 4, p. 326-332.
12. J.G. Semmler, M.A. Nordstrom, A comparison of cross-correlation and surface EMG techniques used to quantify motor unit synchronization in humans, J. Neurosci. Methods 90 (1) (1999) 47–55.
13. A. Kittel, J. Parisi, K. Pyragas, Generalized synchronization of chaos in electronic circuit experiments, Physica D 112 (3–4) (1998) 459–471.
14. X. Zhao, Z. Li, S. Li, Synchronization of a chaotic finance system, Appl. Math. Comput. 217 (3) (2011) 6031–6039.
15. A. Bohn, J. García-Ojalvo, Synchronization of coupled biological oscillators under spatially heterogeneous environmental forcing, J. Theoret. Biol. 250 (1) (2008) 37–47.
16. J. Theiler, Phys. Rev. A 34 (1986) 2427.
17. T. Kreuz, R.G. Andrzejak, F. Mormann, A. Kraskov, H. St¨ogbauer, C.E. Elger, K. Lehnertz, P. Grassberger, Phys. Rev. E 69 (2004) 061915
18. Stam, C.J., van Dijk, B.W., 2002. Synchronization likelihood: an unbiased measure of generalized synchronization in multivariate data sets. Physica D 163, 236–241.

AUTHOR PROFILE

Ayan Mitra is presently a bachelor of Electrical Engineering student from Jadavpur University, Jadavpur, India. He is scheduled to receive his B.E. degree in 2013.He is a recipient of the Human resource merit scholarship for his outstanding marks in higher secondary examination 2009. His undergraduate research work includes i) Designing a data acquisition system using FPGA, ii) Developing a GUI based data acquisition system, iii) Determination of synchronization of EEG Signals by synchronization Likelihood, Visibility Graph similarity, linear correlation, Phase Synchronization, Non-linear interdependencies, Event synchronization, mutual information, v)Design, Fabrication & testing of constant voltage source for heating a filament in cyclotron, vi)speech processing & design of an automated system for displaying voiced letters in text. His area of interest include Power Electronics, Bio-medical Signal Processing and control systems.

Budhaditya Pyne is presently a bachelor of Electrical Engineering student from Jadavpur University, Jadavpur, India. He is scheduled to receive his B.E. degree in 2013.He is a recipient of the Human resource merit scholarship for his outstanding marks in higher secondary examination 2009.His undergraduate research work includes i)Development of Image Processing based biometric authentication(Face Detection),ii) Traffic signal controller using Labview. His area of interest include Instrumentation, Signal Processing and control systems.